

Influence of LV Neutral Grounding on Global Earthing Systems

G. Cafaro*, P. Montegiglio*, F. Torelli*, A. Barresi[‡], P. Colella[§], A. De Simone[†], M. L. Di Silvestre[¶], L. Martirano[¶], E. Morozova[†], R. Napoli[§], G. Parise[¶], L. Parise[¶], E. Pons[§], E. Riva Sanseverino[¶], R. Tommasini[§], F. Tummolillo[‡], G. Valtorta[†] and G. Zizzo[¶]

* Dipartimento di Ingegneria Elettrica e dell'Informazione, Politecnico di Bari, Bari, Italy, giuseppe.cafaro@poliba.it

[†] Enel Distribuzione SpA, Roma, Italy, angelo.desimone@enel.com

[‡] IMQ, Milano, Italy, filomena.tummolillo@imq.it

[§] Dipartimento Energia, Politecnico di Torino, Torino, Italy, pietro.colella@polito.it

[¶] Dipartimento di Energia, Ingegneria dell'Informazione e Modelli Matematici,

Università degli studi di Palermo, Palermo, Italy, gaetano.zizzo@unipa.it

[¶] Dipartimento di Ingegneria Astronautica, Elettrica ed Energetica, Università degli Studi di Roma "La Sapienza", Roma, Italy, luigi.martirano@uniroma1.it

Abstract— International Standards define a Global Earthing System as an earthing net created interconnecting local Earthing Systems (generally through the shield of MV cables and/or bare buried conductors). In Italy the Regulatory Authority for Electricity and Gas requires Distributors to guarantee the electrical continuity of LV neutral conductor. This requirement has led to the standard practice of realizing “reinforcement groundings” along the LV neutral conductor path and at users’ delivery cabinet. Moreover, in urban high load scenarios (prime candidates to be part of a Global Earthing System), it is common that LV distribution scheme creates, through neutral conductors, an effective connection between grounding systems of MV/LV substations, modifying Global Earthing System consistency. Aim of this paper is to evaluate the effect, in terms of electrical safety, of the above mentioned LV neutral distribution scheme when an MV-side fault to ground occurs. At this purpose simulations are carried out on a realistic urban test case and suitable evaluation indexes are proposed.

Keywords—Global Earthing System; GES; Global Grounding System; GGS; Ground potential; Maxwell Sub-areas Method; LV neutral conductor

I. INTRODUCTION

Grounding systems surely are a traditional topic in electrical engineering [1]–[7]. With reference to their quasi-stationary behaviour, the research field could seem fully explored. However, the need of electrical services widespread delivery, along with the significant increase of demand in concentrated areas (i.e. industrial/urban areas), makes it necessary to reconsider some aspects of groundings.

International Standards [8], [9], defining the Global Earthing System (GES), point out how GES advantages result primarily from two aspects:

- grounding systems *Interconnection*;

- *Proximity* of interconnected grounding systems.

GES, in fact, arises from the interconnection between distributors’ (as well as private users’) MV/LV substations Earthing Systems (ES). This interconnection, made (at least) with the metal shield of MV cables, allows the repartition of MV single line to ground fault currents in more than one injection point in the soil [10], [11], thus producing a consistent reduction of Earth Potential Rise (EPR) of the faulted substation.

Proximity effects should avoid the presence of dangerous touch voltages in the considered area (*quasi-equipotentiality* condition).

A full discussion on the above mentioned concepts (*Interconnection*, *Proximity* and *Quasi-equipotentiality*) and their implications can be found in [12].

The Italian Authority prescribes a TT distribution system for LV users [13] and, in its effort to guarantee the best service quality, imposes strict constraints to Distributor System Operators (DSOs) with regards to LV neutral continuity.

As a consequence, LV neutral conductors are grounded (typically with a single grounding rod) at each user delivery cabinet and, sometimes, along their path (neutral *reinforcement groundings*).

In areas characterized by high load, DSOs often reach users delivery nodes with LV lines coming from two different substations (belonging to the same or different feeding stations). This choice is meant to ensure the quickest post-contingency power restore to customers, providing them the opportunity to be fed from different sides. To make LV network radial, lines are disconnected in a distribution box, while neutral conductors are never interrupted, realizing an effective interconnection between substation grounding systems of the considered area.

What above said, along with neutral reinforcement groundings, produces a further increase in the density of the earthing network serving the area, possibly modifying GES consistency.

In this work, developed under the Meterglob Project [14], [15], effects on electrical safety, due to the sole LV neutral interconnections, have been analyzed for an urban area chosen as case study.

This paper was developed as part of the research “METERGLOB”, co-funded by the CCSE (today CSEA, Cassa per i Servizi Energetici Ambientali), with the participation of six partners: ENEL Distribuzione, Istituto Italiano del Marchio di Qualità IMQ, Politecnico di Bari, Politecnico di Torino, Università di Palermo and Sapienza Università di Roma.

Simulations have been carried out with a software, written in Matlab, which passed experimental testing [16].

The Meterglob Project, cofounded by the Italian CCSE (Cassa Conguaglio per il Settore Elettrico), is investigating on different aspects related to GES, in particular on the contribution of extraneous conductive parts [15] and on the problem of periodic testing of ESs reliability [17].

The Project main purpose is supporting Standardization Bodies in providing a more precise definition of GES as well as reliable procedures to assess and verify GES existence. In line with this target, suitable indexes for the evaluation of electrical safety degree of the area under investigation have been evaluated.

This work was presented at the 2015 IEEE 15th International Conference on Environment and Electrical Engineering, Rome, Italy, June 10-13 [18].

II. THE MODEL

The system under investigation, which is hereafter referred to as “*Total System*”, is depicted in Fig. 3. It is a simplified representation of a typical urban scenario, potentially candidate to be defined as a portion of a GES.

In this section its mathematical model is reported, after a brief recall of the Maxwell Sub-Areas Method theoretical background.

A detailed description of all Total System components is presented in Section III.

A. Grounding Systems Quasi-stationary Model

The study of a grounding electrode leaking a known quasi-stationary current (50-60 Hz) can be accomplished applying the Maxwell Subareas Method (MaSM) [1], [7], [19], [20].

The method is based on subdividing the leaking surface of the considered electrode in a suitable number n of smaller portions (subareas) having the following characteristics:

1. to be small enough to consider their surface leakage current density uniform;
2. to have a shape that allows to find an analytical expression of their produced field and potential when considered alone in an uniform, isotropic and indefinite medium;
3. to be at the same potential under fault conditions.

Statement 3 means that the voltage drop across the metal parts of the electrode is negligible, which is an amply justified hypothesis considering that the conductivity of electrodes parts is considerably greater than the soil one.

Fig. 1 shows an example of discretization of a simple cylindrical electrode embedded in a conductive homogeneous medium (the formulation extension to more complex geometries is immediate).

According to the MaSM, it has been subdivided in n cylindrical segments that satisfy condition 1 but still have a length adequately greater than their diameter ($2r/L \ll 1$), in order to assume the current field generated by each of them the same as that produced by uniform linear current sources laying on their longitudinal axes.

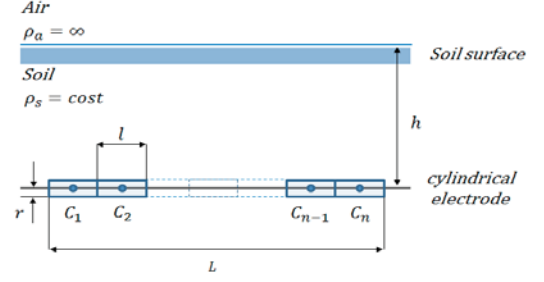


Fig. 1. Example of discretization of a simple cylindrical conductor

Every single subarea interferes with the others by means of *voltage coefficients* R_{ij} ($i, j = 1, 2, \dots, n$) which represent the voltage produced by the generic inducing subarea j in the C_i barycentre of the induced subarea i , when j is leaking a unitary current. Being ρ the resistivity of the considered uniform medium, the analytical expression of the generic voltage coefficient is:

$$R_{ij} = \frac{\rho}{4\pi l_j} \ln \left[\frac{x_i + \frac{l_j}{2} + \sqrt{\left(x_i + \frac{l_j}{2}\right)^2 + y_i^2 + z_i^2}}{x_i - \frac{l_j}{2} + \sqrt{\left(x_i - \frac{l_j}{2}\right)^2 + y_i^2 + z_i^2}} \right] \quad (1)$$

where $l_j = L/n$ is the length of the inducing subarea and (x_i, y_i, z_i) are the coordinates of C_i on a local coordinate system centered on C_j . When $i = j$, expression (1) allows the evaluation of the *self-induced voltage coefficient* R_{ii} by the following substitutions: $y_i = z_i = 0$ and $x_i = r$, where r is the radius of the considered conductor.

The application of the MaSM method leads, for a single grounding electrode leaking a known current I_F , to the formulation of the following set of linear equations:

$$\begin{cases} R_{i1}I_1 + R_{i2}I_2 + \dots + R_{in}I_n = V_i = V_E & i = 1, 2, \dots, n \end{cases} \quad (2)$$

$$I_1 + I_2 + \dots + I_n = I_F \quad (3)$$

where V_i is the potential assumed by each sub-area.

Equation set (2)-(3) solution gives the n subcurrents I_j leaked by each subarea and the Earth Potential Rise V_E of the considered electrode. The knowledge of subcurrent I_j allows the subsequent computation of the electric potential at any point of the soil surface.

The presence of air in half of the space domain, as well as the presence in the medium of layers with different resistivity (multi-layer soil model), is taken into account by means of the electrical images principle [1], [20].

Since each subarea is modelled as a uniform linear current source, it is obvious that a larger number of them results in a more adequate representation of the leakage current distribution along the electrode. Simulations reported in this paper have been repeated increasing n until negligible variations on ground surface potential values ($< 1\%$) have been observed.

B. Long Buried Conductors Quasi-stationary Model

As above said, MaSM operates under the assumption of equipotentiality for grounding electrodes in quasi-stationary condition. This hypothesis leads to results whose accuracy degree decreases with increasing of electrodes dimension (e.g. long buried metal pipes, railways, etc.), being the voltage drop along them no more negligible [3].

It is possible to extend the applicability of MaSM to the case of a long buried conductor [21]. With reference to Fig. 2, once subdivided the considered electrode in n subareas (trunks), each of them have to be considered as a separate grounding electrode, connected to the trunks immediately before and after by means of an admittance.

It is well known that, at industrial frequency, the interference phenomenon between bare conductors in contact with the soil can be described with satisfactory accuracy through purely resistive parameters [3]. Therefore, the admittance that connects consecutive trunk barycentres can be substituted by a conductance, whose value is given by the material and section of the conductor itself.

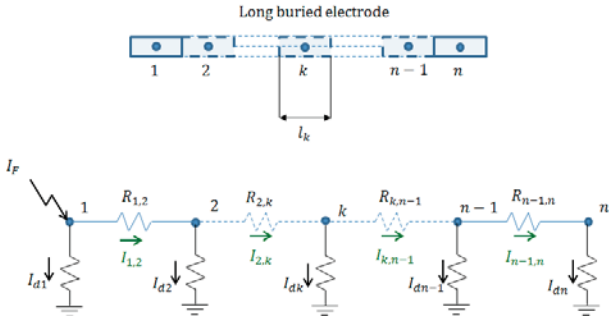


Fig. 2. Long bare buried electrode model

Currents flowing from a subarea to the neighbouring ones became new variables and can be determined, as well as the leakage current distribution along conductors.

C. Total System Model

With reference to Fig. 3, *Total System* is composed by $N_{MV} = 3$ MV/LV substation grounding electrodes connected each other and with $N_r = 37$ grounding rods (neutral *reinforcement groundings*) through the LV distributed neutral conductor. In the area under investigation there are also $N_{LV} = 33$ LV users grounding electrodes (TT system) and $N_p = 3$ distinct pipelines (extraneous conductive parts). Both N_{MV} and N_{LV} grounding electrode plan view geometries are square, as reported in Fig. 3.

Naming:

- $N_{gs} = N_{MV} + N_{LV}$;
- $n_{gstot} = \sum_{i=1}^{N_{gs}} n_{gs_i}$, where n_{gs_i} is the subareas number of the i^{th} grounding system;
- $n_{rtot} = \sum_{i=1}^{N_r} n_{r_i}$, where n_{r_i} is the subareas number of the i^{th} grounding rod;
- $n_{ptot} = \sum_{i=1}^{N_p} n_{p_i}$, where n_{p_i} is the subareas number of the i^{th} pipeline;

- $n_{l_{LV}}$ the number of grounding electrodes connection sections realized by LV neutral conductor (Fig. 3); and being:
- $\mathbf{V}_{gs} = [V_{gs_1}, \dots, V_{gs_{N_{gs}}}]^T$ the unknown vector of EPRs assumed by the *Total System* square grounding electrodes;
- $\mathbf{V}_r = [V_{r_1}, \dots, V_{r_{N_r}}]^T$ the unknown vector of EPRs assumed by *Total System* grounding rods;
- $\mathbf{V}_{p_i} = [V_{p_i,1}, \dots, V_{p_i,n_{p_i}}]^T$ ($i = 1, \dots, N_p$) the unknown vector of EPRs assumed by the n_{p_i} subareas of the i^{th} pipeline;
- $\mathbf{Id}_{gs_i} = [Id_{gs_i,1}, \dots, Id_{gs_i,n_{gs_i}}]^T$ ($i = 1, \dots, N_{gs}$) the unknown vector of subcurrents leaked by the i^{th} grounding electrode subareas;
- $\mathbf{Id}_{r_i} = [Id_{r_i,1}, \dots, Id_{r_i,n_{r_i}}]^T$ ($i = 1, \dots, N_r$) the unknown vector of subcurrents leaked by the i^{th} grounding rod subareas;
- $\mathbf{Id}_{p_i} = [Id_{p_i,1}, \dots, Id_{p_i,n_{p_i}}]^T$ ($i = 1, \dots, N_p$) the unknown vector of subcurrents leaked by the i^{th} pipeline subareas;
- $\mathbf{I}_{l_{LV}}$ the unknown vector of currents flowing through the $n_{l_{LV}}$ connection sections between grounding electrodes;
- $\mathbf{I}_{l_{p_i}} = [I_{l_{p_i,1}}, \dots, I_{l_{p_i,n_{p_i}-1}}]^T$ ($i = 1, \dots, N_p$) the unknown vector of currents flowing along the trunks of the i^{th} pipeline (with reference to Fig. 2);

the *Total System* model, which describes both the effects of mutual interferences due to current fields established in the ground and the presence of LV neutral connections, can be expressed as follows:

$$\begin{cases} \mathbf{U}\mathbf{x}_1 - \mathbf{R}\mathbf{x}_2 = \mathbf{0} & (4) \\ \mathbf{F}\mathbf{x}_2 + \mathbf{A}\mathbf{x}_3 = \mathbf{I}_{k_1} & (5) \\ \mathbf{M}\mathbf{x}_1 - \mathbf{x}_3 = \mathbf{0} & (6) \\ \mathbf{U}_s\mathbf{x}_2 = \mathbf{I}_{k_2} & (7) \end{cases}$$

where:

- $\mathbf{x}_1 = [\mathbf{V}_{gs}^T, \mathbf{V}_r^T, \mathbf{V}_{p_1}^T, \dots, \mathbf{V}_{p_{N_p}}^T]^T$;
- $\mathbf{x}_2 = [\mathbf{Id}_{gs_1}^T, \dots, \mathbf{Id}_{gs_{N_{gs}}}^T, \mathbf{Id}_{r_1}^T, \dots, \mathbf{Id}_{r_{N_r}}^T, \mathbf{Id}_{p_1}^T, \dots, \mathbf{Id}_{p_{N_p}}^T]^T$;
- $\mathbf{x}_3 = [\mathbf{I}_{l_{LV}}^T, \mathbf{I}_{l_{p_1}}^T, \dots, \mathbf{I}_{l_{p_{N_p}}}^T]^T$.
- $\mathbf{U} = \text{blockdiag}(\mathbf{U}_{gs_1}, \dots, \mathbf{U}_{gs_{N_{gs}}}, \mathbf{U}_{r_1}, \dots, \mathbf{U}_{r_{N_r}}, \mathbf{U}_p)$, with $\mathbf{U}_{gs_i} = [1, 1, \dots, 1_{n_{gs_i}}]^T$, $\mathbf{U}_{r_i} = [1, 1, \dots, 1_{n_{r_i}}]^T$ and $\mathbf{U}_p = \text{diag}([1, 1, \dots, 1_{n_{p_{tot}}}]$;
- \mathbf{R} is the $(n_{tot} \times n_{tot})$ matrix of voltage coefficients, with $n_{tot} = n_{gstot} + n_{rtot} + n_{ptot}$;
- $\mathbf{F} = \text{blockdiag}(\mathbf{F}_{LV}, \mathbf{U}_p)$, where \mathbf{F}_{LV} is equal to \mathbf{U}^T matrix curtailed of the $N_{LV} + n_{p_{tot}}$ lines corresponding to grounding electrodes not connected to the LV neutral network;

- $\mathbf{A} = \text{blockdiag}(\mathbf{A}_{LV}, \mathbf{A}_{PT})$, where \mathbf{A}_{LV} is the node-lines matrix of LV neutral network in Fig. 6 (excluding the remote earth node and its afferent lines) and $\mathbf{A}_{PT} = \text{blockdiag}(\mathbf{A}_{p1}, \mathbf{A}_{p2}, \dots, \mathbf{A}_{pN_p})$ where \mathbf{A}_{p_i} is the node-lines incidence matrix of the resistive network represented in Fig. 2, written, for each pipe, excluding the remote earth node and its afferent lines;
- \mathbf{I}_{k_1} is the known vector of injected currents in LV neutral network nodes (it has $N_{MV} + N_r$ elements);
- $\mathbf{I}_{k_2} = [\mathbf{I}_{k_1}, \dots, \mathbf{I}_{k_{N_{LV}}}, \mathbf{I}_{k_{p_1}}^T, \dots, \mathbf{I}_{k_{p_{N_p}}}^T]^T$, where \mathbf{I}_{k_i} is the known leaked current of i^{th} grounding electrode not connected to Fig. 6 network (equal to zero for passive elements) and $\mathbf{I}_{k_{p_i}}$ is the known vector of currents injected in subareas barycentres of the i^{th} pipeline (nodes of resistive network in Fig. 2);
- \mathbf{U}_s is equal to \mathbf{U}^T matrix curtailed of lines corresponding to the N_{MV} grounding electrodes connected to the LV neutral network.

Matrix \mathbf{M} in (6), has the following structure:

$$\mathbf{M} = \begin{bmatrix} \mathbf{M}_1 \\ \mathbf{M}_2 \end{bmatrix} = \begin{bmatrix} \text{diag}(\mathbf{Y}_N) \mathbf{M}_{LV}^T & \mathbf{0} \\ \mathbf{0} & \text{diag}(\mathbf{G}) \mathbf{A}_{PT}^T \end{bmatrix} \quad (8)$$

where:

- \mathbf{Y}_n is the vector of neutral connections admittances;
- $\mathbf{G} = [\mathbf{G}_1, \dots, \mathbf{G}_{N_p}]^T$, where \mathbf{G}_i is the vector of the conductances connecting the subareas barycentres of the i^{th} pipe (with reference to Fig. 2);
- \mathbf{M}_{LV}^T is the line-nodes matrix for the LV neutral network, written so that the size and the sort order of its columns are congruent with vector $[\mathbf{V}_{gs}^T, \mathbf{V}_r^T]^T$.

Since \mathbf{I}_{k_1} , \mathbf{I}_{k_2} and \mathbf{Y}_N are, in general, complex quantities, \mathbf{x}_1 , \mathbf{x}_2 and \mathbf{x}_3 will be such also.

By decomposing each of the (4)-(7) equations in their real and imaginary parts, all the relations needed for a unique direct solution are provided.

Due to the short connections, capacitive couplings between LV neutral conductor and remote earth, LV and MV lines are considered negligible and not taken into account. Inductive couplings between LV neutral conductor MV and LV lines are also neglected.

III. CASE STUDY

Fig. 3 reports a plan view of the implemented case study, which is a simplified schematization of a real urban district portion in Torino, composed by six city blocks [16].

According to the requirements for the automatic disconnection of supply given by the international Standard IEC 60364-4 [22] for TT systems (the unique possible for LV users in Italy), each building of each block has an ES disjointed

from the MV/LV substations' ones (squares in red dotted lines). The ESs of LV users, as well as the ESs of the MV/LV substations, are modeled with a square electrode, buried at 0.5 m under the soil level. The ES of the faulted MV/LV substation is the number 21.

The total fault current is $I_F = 100 \angle 0.00$ [A], typical for a single line to ground fault in an Italian urban scenario (isolated neutral MV distribution system).

Blue lines represent three distinct water pipes, buried at 1 m (dashed line) and 1.3 m (dot-dash lines) depths.

The soil has been considered homogeneous, characterized by a resistivity of $100 \Omega m$. As shown in Table I [9], this value can be considered representative of loam/clay/humus soil.

TABLE I
TYPICAL SOIL RESISTIVITY RANGES
PROVIDED BY EN 50522 (ANNEX J)

Type of soil	Soil resistivity [Ωm]		
Marshy soil	5	to	40
Loam, clay, humus	20	to	200
Sand	200	to	2500
Gravel	2000	to	3000
Weathered rock	mostly below		1000
Sandstone	2000	to	3000
Granite		up to	50000
Moraine		up to	30000

Other geometrical and electrical details are reported in Table II.

Simulations goal is to evaluate how the presence of distributed LV neutral conductor (green solid lines in Fig. 3) and its "reinforcement grounding rods" (concentric circles in Fig. 3) modify both the electric potential profile (EPP) on the soil surface and the Transferred Potential (TP) on floating metallic parts.

One of the main concerns regarding electrical safety is the evaluation of the prospective touch voltage, which is defined as "*the voltage between simultaneously accessible conductive parts when those conductive parts are not being touched*" [9]. A typical case is related to the voltage between a metallic object and the soil surface. This is the case analyzed here: a human being that could touch the energized metallic object while standing in its vicinity (reasonably in a limited region close to the metallic object).

For this reason, limited soil surface areas called Inspection Areas (IAs) have been identified above each grounding electrode and all along pipelines. As an example, Fig. 3 reports the IA associated to grounding electrode 18 (which is similar for all square grounding electrodes) and the IA considered along one of the pipelines (areas below blue dashed line hatch). Within these IAs, the maximum prospective touch voltage can be evaluated as the difference between the metallic object's potential and the minimum soil surface potential in the area.

Table II also reports IAs geometrical parameters.

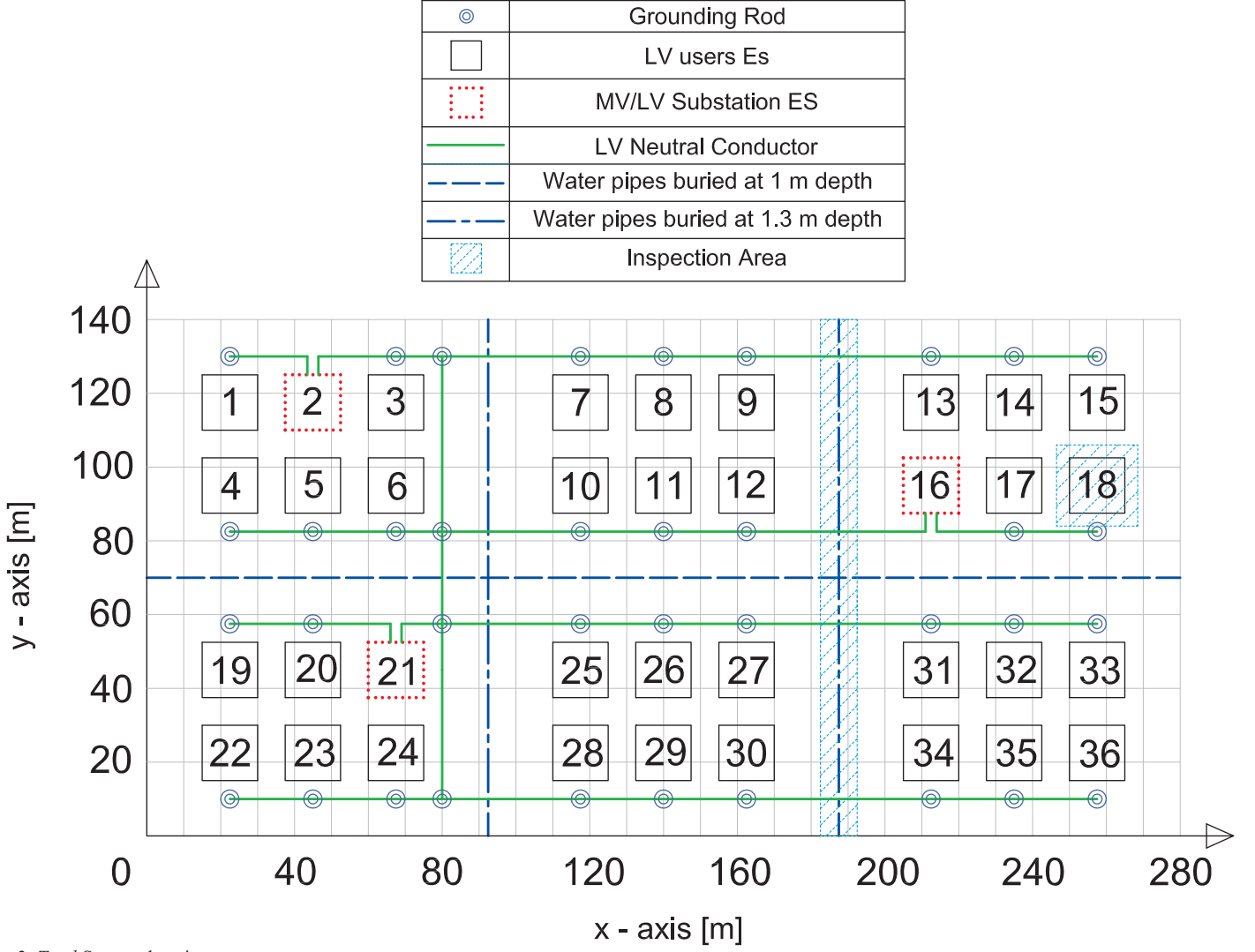


Fig. 3. Total System plan view

TABLE II
GEOMETRICAL AND ELECTRICAL DETAILS OF THE CASE STUDY

Symbol	Quantity	Values
L_{SE}	Square electrodes length	15 m
L_{GR}	Grounding rod length	1.5 m
L_{IALV}	Length of square Inspection Area around the j^{th} LV ES	22 m
L_{IAP}	Thickness of Inspection Area along pipes	7 m
r_{SE}	Square electrode conductor radius	4 mm
r_{GR}	Grounding rod radius	10 mm
r_{WP}	Water pipes radius	50 mm
r_{LV}	LV neutral conductor radius	3.99 mm
\hat{z}_{LV}	LV neutral conductor impedance	$0.393+j0.101 \Omega/\text{km}$
g_{WP}	Water pipes conductance	$1.555 \text{ S}\cdot\text{km}$

Two scenarios have been considered:

- Scenario 1: LV neutral connections and reinforcement grounding rods missing. Faulted MV/LV substation is called to disperse the entire fault current I_F ;
- Scenario 2: Total system as represented in Fig. 3.

For each scenario the fault current is kept constant.

To carry out the comparison, together with contour plots of the ground potential, three shape coefficients have been evaluated on the same portion of soil surface: Uniformity (C_U), Valley Effect (C_{VE}), Gradient (C_G):

$$C_U = \frac{|V_{AV}|}{|V_{MAX}|} \quad (9)$$

$$C_{VE} = \frac{|V_{MIN}|}{|V_{AV}|} \quad (10)$$

$$C_G = \max(|\nabla V(x,y)|) \quad (11)$$

where:

- V_{AV} = EPP Average Value;

- V_{MAX} = EPP Maximum Value;
- V_{MIN} = EPP Minimum Value;
- $\nabla V(x, y)$ = EPP gradient.

These coefficients allow a global evaluation of EPP on the area under investigation.

In order to evaluate electrical safety degree for each scenario, the Maximum Touch Voltage coefficient (C_{MTV}) has been introduced:

$$C_{MTV} = \frac{V_{TMax}}{|EPR_{21}|} = \frac{(|V_{TPj} - V_{IAminj}|)_{Max}}{|EPR_{21}|} \quad (12)$$

where:

- EPR_{21} = EPR of MV/LV faulted substation ES;
- V_{TPj} = TP on the j^{th} Floating Part;
- V_{IAminj} = Minimum Voltage (with respect to remote earth) of the Soil in the Inspection Area around the j^{th} LV ES and along pipes (with reference to Fig. 3).

Coefficients C_U , C_{VE} , and C_{MTV} can be considered independent from the product of the soil resistivity to the fault current (as will be shown in Subsection III.A). They allow for considerations that are valid for different kind of soil and different fault current values. Coefficient C_G instead depends on the product ρI_F ; however, by comparing the results for the two scenarios, that are simulated with the same values of soil resistivity and fault current, qualitative conclusions with general validity can be obtained.

Finally, a computation of the maximum fault current, for which users' safety requirement (13) is satisfied, has been performed for each scenario.

$$V_{TMax} \leq 50V \quad (13)$$

The utilized relation is the following:

$$|I_{50Vj}| = \frac{50}{C_{MTV} \cdot R_{eqj}} \quad j = 1, 2 \quad (14)$$

where R_{eq} is defined as the ratio of $|EPR_{21}|$ to total fault current I_F modulus.

A. Simulation results

Fig. 4 and Fig. 5 show the EPP contour plots for both the simulated scenarios. They allow to qualitatively evaluate the equipotentialization effect of the grounding network (interconnected MV/LV ESs and LV neutral reinforcement groundings). Table III reports, for each simulated scenario, the MV/LV substations EPRs and all the quantities presented in the previous section. EPRs' phase angles are expressed in degree. Scenario 2 reports a drastic reduction of faulted substation EPR (about 77%). This is due to the distribution of the fault current between all other grounding electrodes connected through LV neutral conductor. As reported in Fig. 6, faulted substation is in fact called on to disperse less than 20% of the total fault current.

As explained in Section II, the implemented model takes into account both the real and the imaginary part of the LV neutral

connection impedances. From Fig. 6, it can be observed that the phase angle differences among the currents leaked by the earthing electrodes are negligible. This means that the model, in case of short connections, can be simplified not taking into account LV connection inductances.

The great increase of uniformity coefficient C_U from scenario 1 to scenario 2 is obviously due to the above mentioned reduction of EPR_{21} , but also to the rise of EPP in areas far from the faulted substation (thanks to currents leaked by all auxiliary electrodes).

Same considerations can be made about the smaller increase of C_{VE} .

Particularly significant is the reduction of the maximum EPP gradient modulus (about 80%), which is a relevant index of the equipotentiality degree reached by the area under investigation.

TABLE III
EPR AND SHAPE COEFFICIENTS FOR THE SIMULATED SCENARIOS

Quantity	Scenario N°	
	1	2
$EPR_2^* [V^\circ]$	19.6 ^{±0.0}	84.5 ^{±0.1}
$EPR_{16}^* [V^\circ]$	13.6 ^{±0.0}	84.1 ^{±0.2}
$EPR_{21} [V^\circ]$	379.2 ^{±0.0}	86.2 ^{±0.2}
C_U	0.091	0.347
C_{VE}	0.330	0.481
$C_G [V/m]$	70.327	13.184

*in scenario 1 it corresponds to a transferred potential

Table IV reports the shape coefficients recalculated for a single block of the urban area, the one containing the faulted substation.

TABLE IV
SHAPE COEFFICIENTS FOR A SINGLE BLOCK

Quantity	Scenario N°	
	1	2
C_U	0.214	0.395
C_{VE}	0.325	0.500
$C_G [V/m]$	70.327	13.184

Uniformity coefficient C_U , calculated for the reduced area, is obviously different from that calculated before. The maximum voltage is in fact the same, while the average is greater (low far-away potential are not considered). As expected, the C_U increase is smaller for scenario 2.

Coefficient C_{VE} remains the same, being both average and minimum values increased. The unchanged value of C_G states that, for each scenario, maximum step voltages are located in proximity of the faulted substation.

Table V reports quantities introduced to evaluate TPs on floating parts and touch voltages.

Quantity V_{TPMax} is the modulus, expressed in percentage of EPR_{21} , of the maximum transferred potential to floating parts. It is nearly doubled in scenario 2, as a consequence of the diffused presence of active electrodes around floating parts (higher couplings due to the current field in the soil).

Coefficient C_{MTV} remains practically the same. This means that also the ratio of minimum soil potential (even if evaluated for different inspection areas) to the EPR of faulted station has increased. With reference to absolute touch voltages, this means a general improvement of considered area electrical safety from a scenario to another.

TABLE V
EVALUATION OF TRANSFERRED POTENTIAL

Quantity	Scenario N°	
	1	2
$V_{TP_{max}} [\%]$	18.70 (on ES 24)	35.01 (on ES 5)
C_{MTV}	0.0757 (IA above ES 20)	0.0790 (IA above ES 1)
$ I_{50V} [A]$	173.6	733

Current I_{50V} modulus can be taken as an indicator of electrical safety degree, with reference to LV users. Results reported in Table V confirms that scenario 2 is four times safer than scenario 1.

Table VI reports the values of the coefficients C_U , C_{VE} and C_G evaluated, for both the considered scenarios, keeping the fault current constant and varying the soil resistivity. Table VII shows the same quantities evaluated, for different values of the fault current, assuming two different soil resistivity values: 10 Ωm and 1000 Ωm .

The comparison with Table III shows, in both the scenarios, differences in the first two shape coefficients that can be considered negligible.

C_U and C_{VE} (as well as C_{MTV}) are defined as the ratios of quantities having the same proportionality relation with the product ρI_F . When galvanic interconnections among ground

electrodes are absent, their independence from soil resistivity and fault current is rigorous [20].

The case study considered in this work presents, in both the simulated scenarios, galvanic interconnections among some of the ground electrodes considered. In Scenario 1, conductances between adjacent pipeline trunks have been introduced in order to properly represent long buried conductors; in Scenario 2, there is also the LV neutral network.

The differences in C_U and C_{VE} values reported in Table III, VI and VII are due to the slight changes of the fault current distribution between the soil and the galvanic interconnections in the different considered conditions.

It can be concluded that the results of this study are generally valid also for different values of the product ρI_F .

TABLE VI
SHAPE COEFFICIENTS FOR DIFFERENT SOIL RESISTIVITY

$I_F [A]$	Scenario	$\rho [\Omega m]$	C_U	C_{VE}	$C_G [V/m]$
100	1	10	0.090	0.319	7.030
		1000	0.090	0.332	703.340
	2	10	0.314	0.478	1.510
		1000	0.352	0.482	133.148

TABLE VII
SHAPE COEFFICIENTS FOR DIFFERENT FAULT CURRENTS

$\rho [\Omega m]$	Scenario	$I_F [A]$	C_U	C_{VE}	$C_G [V/m]$
10	1	10	0.090	0.319	0.703
		1000	0.090	0.319	70.305
	2	10	0.314	0.478	0.151
		1000	0.314	0.478	15.099
1000	1	10	0.090	0.332	70.334
		1000	0.090	0.332	7.033·10 ³
	2	10	0.352	0.482	13.315
		1000	0.352	0.482	1.331·10 ³

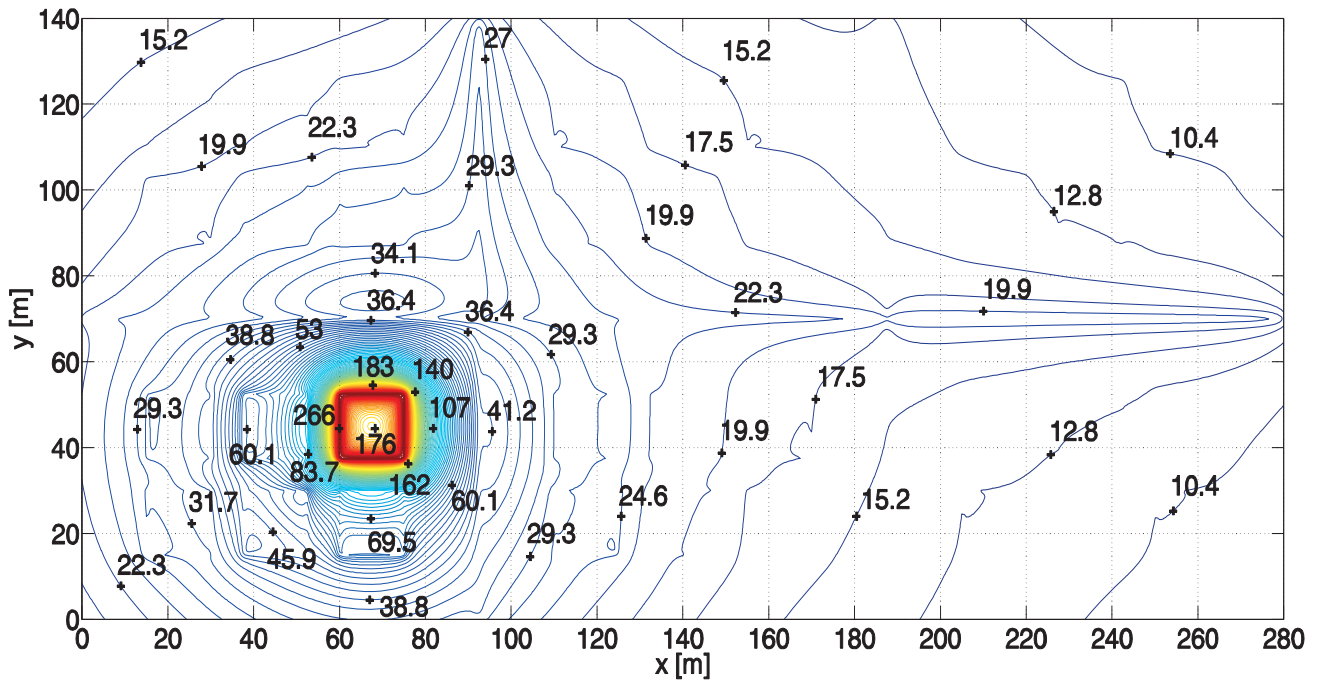


Fig. 4. EPP contour plot (in volt) for scenario 1

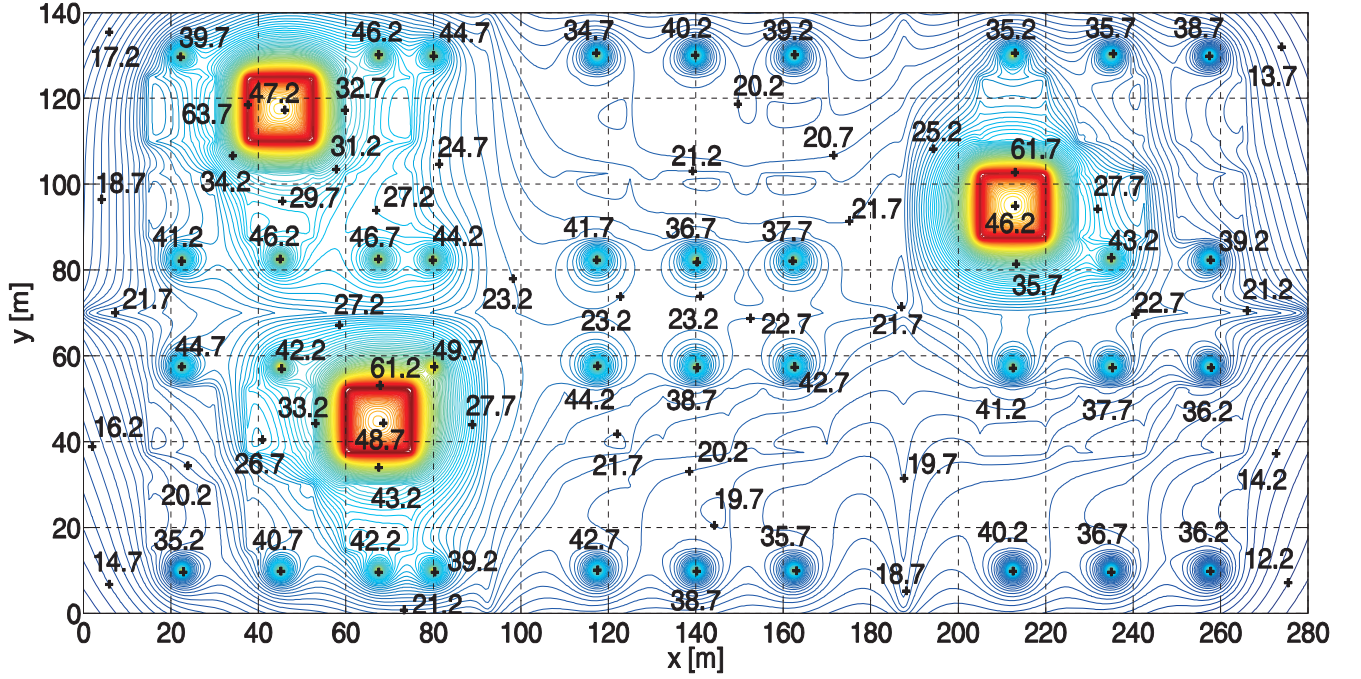


Fig. 5. EPP contour plot (in volt) for scenario 2

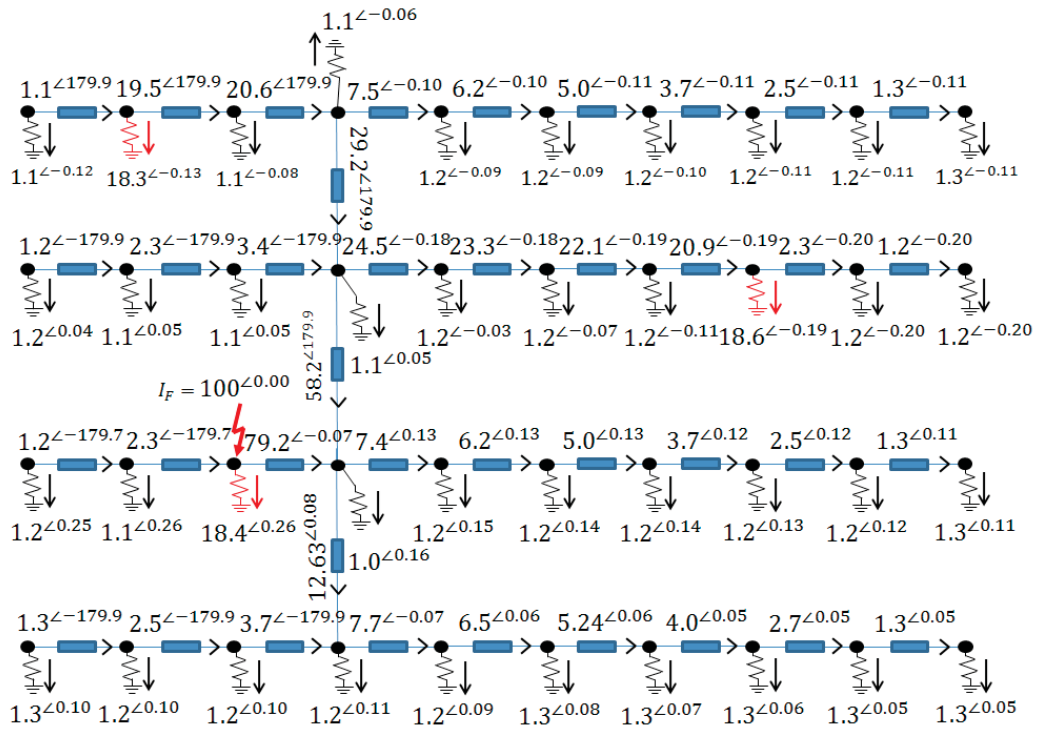


Fig. 6. Scenario 2: LV neutral network current flows (modulus in ampere, phase angle in degree). Red resistances correspond to MV/LV substations ES.

IV. CONCLUSIONS

This work analyzes the role, in electrical safety, of the LV distributive scheme adopted in Italy for high load areas.

At this purpose the effect of the sole presence of LV neutral interconnections between substations ESs, along with LV

neutral reinforcement groundings, have been evaluated in case of a MV single line to ground fault.

With reference to the worst case scenario (faulted substation called on to disperse the entire fault current), simulation results show an EPR reduction of 77% in the faulted substation. The

interconnection between grounding electrodes determines a modification in the soil surface voltage distribution. Even if a voltage increase can be observed in areas where scenario 1 exhibited low potentials (far from MV/LV substations), scenario 2 shows a significant decrease of the maximum touch voltage and EPP gradients detectable in the area under investigation.

This is because the described LV distributive scheme realizes, although in a small area, all the concepts behind the Standards' GES definition: *Interconnection*, *Proximity* and *Quasi-equipotentiality*. For this reasoning it surely improves GES efficiency in that area and its realization should be recommended.

REFERENCES

- [1] P. Buccheri, V. Cataliotti, G. Morana, "Caolcolo automatico di impianti di terra comunque complessi in terreni omogenei e non omogenei a doppio strato," *Energ. Elettr.*, pp. 293-304, 1977.
- [2] J. M. Nahman, "Analysis of interconnected earthing systems", *Archiv fur Elektrotechnik*, No. 63, pp. 261-265, 1981.
- [3] G. Ala, P. Buccheri, A. Campoccia, "Interferenza tra elettrodi interrati rettilinei a caduta di tensione longitudinale non trascurabile. Analisi dell'accoppiamento conduttivo," *Energ. Elettr.*, No. 10, pp. 405-413, 1992.
- [4] J. C. Maxwell, *A Treatise On Electricity and Magnetism*, vol. 2. New York, NY, USA: Dover, 1954.
- [5] RUDENBERG, R.: 'Transient performance of electric power systems' (McGraw-Hill, 1950).
- [6] E. D. Sunde, *Earth Conduction Effects in Transmission Systems*. New York, NY, USA: Dover, 1968.
- [7] M. Sylos Labini, A. Covitti, G. Delvecchio, and C. Marzano, "A study for optimizing the number of subareas in the Maxwell's method," *IEEE Trans. Magn.*, vol. 39, no. 3, pp. 1159-1162, May 2003.
- [8] *Power installations exceeding 1kV a.c., Part 1: Common rules*. EN 61936-1, 2011.
- [9] *Earthing of power installations exceeding 1 kV a.c.* EN 50522, 2011.
- [10] P. Colella, R. Napoli, E. Pons, R. Tommasini, A. Barresi, G. Cafaro, A. De Simone, M.L. Di Silvestre, L. Martirano, P. Montegiglio, E. Morozova, G. Parise, L. Parise, E. Riva Sanseverino, F. Torelli, F. Tummolillo, G. Valtorta, and G. Zizzo, "Current and Voltage Behaviour During a Fault in a HV/MV System: Methods and Measurements," in *proceedings of Environment and Electrical Engineering (EEEIC)*, 2015 IEEE 15th International Conference on, 2015, pp. 404-409.
- [11] P. Colella, R. Napoli, E. Pons, R. Tommasini, A. Barresi, G. Cafaro, A. De Simone, M.L. Di Silvestre, L. Martirano, P. Montegiglio, E. Morozova, G. Parise, L. Parise, E. Riva Sanseverino, F. Torelli, F. Tummolillo, G. Valtorta, and G. Zizzo, "Currents Distribution During a Fault in an MV Network: Methods and Measurements," *Industry Applications, IEEE Transactions on*, to be published.
- [12] G. Cafaro, P. Montegiglio, F. Torelli, P. Colella, R. Napoli, E. Pons, R. Tommasini, A. De Simone, E. Morozova, G. Valtorta, A. Barresi, F. Tummolillo, A. Campoccia, M. L. Di Silvestre, E. Riva Sanseverino, G. Zizzo, L. Martirano, G. Parise, and L. Parise, "The global grounding system: Definitions and guidelines," in *proceedings of Environment and Electrical Engineering (EEEIC)*, 2015 IEEE 15th International Conference on, 2015, pp. 537-541.
- [13] IEC *Electrical Installations for Buildings – Part 1: Fundamental principles, assesment of general characteristics, definitions*, IEC TS 60364-1:2005
- [14] R. Napoli, R. Tommasini, E. Pons, P. Colella, G. Parise, L. Martirano, L. Parise, A. Campoccia, G. Zizzo, and M. L. Di Silvestre, "The Meterglob Project: Impact of fault current division and of extraneous conductive parts on Global Earthing Systems," in *Proceedings of International Conference on Grounding and Earthing & 6th International Conference on Lightning Physics and Effects*, Manaus, Brazil, 2014.
- [15] G. Cafaro, P. Montegiglio, F. Torelli, "The Meterglob Project," 1th SCORE@POLIBA2014, 3-5 December, Bari, Italy, 2014.
- [16] E. Pons, P. Colella, R. Tommasini, R. Napoli, P. Montegiglio, G. Cafaro, and F. Torelli, "Global Earthing Systems: Can buried metallic structures significantly modify the ground potential profile?," *IEEE Trans.on Industry Applications*, vol. 51, Issue 6, pp. 5237-5246, 2015.
- [17] G. Parise, L. Martirano, L. Parise, F. Tummolillo, G. Vagnati, A. Barresi, G. Cafaro, P. Colella, M. L. Di Silvestre, P. Montegiglio, E. Morozova, R. Napoli, E. Pons, E. Riva Sanseverino, S. Sassoli, R. Tommasini, F. Torelli, G. Valtorta, and G. Zizzo, "A Practical Method to Test the Safety of HV/MV Substation Grounding Systems," in *proceedings of Environment and Electrical Engineering (EEEIC)*, 2015 IEEE 15th International Conference on, 2015, pp. 502-506.
- [18] G. Cafaro, P. Montegiglio, F. Torelli, A. Barresi, P. Colella, A. De Simone, M. L. Di Silvestre, L. Martirano, E. Morozova, R. Napoli, G. Parise, L. Parise, E. Pons, E. Riva Sanseverino, R. Tommasini, F. Tummolillo, G. Valtorta and G. Zizzo, "Influence of LV Neutral Grounding on Global Earthing Systems," in *proceedings of Environment and Electrical Engineering (EEEIC)*, 2015 IEEE 15th International Conference on, 2015, pp. 389-394.
- [19] F. Freschi, M. Mitolo, and M. Tartaglia, "An Effective Semianalytical Method for Simulating Grounding Grids," *Industry Applications, IEEE Transactions on*, vol. 49, no. 1, pp. 256-263, 2013.
- [20] V. Cataliotti and A. Campoccia, *Impianti di terra*. TNE, 2013.
- [21] M. Bronzini, G. Delvecchio, N. Mitaritonna, P. Pugliese, M. Sylos Labini, "A method for studying the current field generated by interconnected grounding systems," 21th ISEF International Symposium on Electromagnetic Field in Electrical Engineering, Maribor, Slovenia, 2003.
- [22] *Low-voltage electrical installations - Part 4-41: Protection for safety - Protection against electric shock*. IEC 60364-4, 2005.